BIOCELL
2023 47(4): 919-928

Tech Science Press

In vitro polymerization of the dopamine-borate melanin precursor: A proof-of-concept regarding ^{10}boron neutron-capture therapy for melanoma†

Juan C. STOCKERT[1,2,*]; Silvina A. ROMERO[1]; Marcelo N. FELIX-POZZI[3]; Alfonso BLÁZQUEZ-CASTRO[4]

[1] Instituto de Oncología "Angel H. Roffo", Área Investigación, Facultad de Medicina, Universidad de Buenos Aires, Buenos Aires, C1417DTB, Argentina
[2] Centro Integrativo de Biología y Química Aplicada, Universidad Bernardo O'Higgins, Santiago, 8370854, Chile
[3] Departamento de Micro y Nanotecnología, Instituto de Nanociencias y Nanotecnología, Centro Atómico Constituyentes, Comisión Nacional de Energía Atómica, Buenos Aires, CP 1650, Argentina
[4] Departamento de Biología, Universidad Autónoma de Madrid, Madrid, 28049, Spain

Key words: ^{10}Boron, Borate esters, Catechols, Dopamine, Eumelanin, Melanoma

Abstract: The ^{10}boron neutron-capture therapy (BNCT) is an emerging antitumoral method that shows increasing biomedical interest. BNCT is based on the selective accumulation of the ^{10}boron isotope within the tumor, which is then irradiated with low-energy thermal neutrons, generating nuclear fission that produces ^{7}lithium, ^{4}helium, and γ rays. Simple catechol-borate esters have been rather overlooked as precursors of melanin biosynthesis, and therefore, a proof-of-concept approach for using dopamine-borate (DABO) as a suitable boron-containing candidate for potential BNCT is presented here. DABO can spontaneously oxidize and autopolymerize *in vitro*, giving a soluble, eumelanin-like brown-black poly-DABO product. Melanotic melanoma cell cultures treated with 1 mM DABO for 24 and 48 h were viable and showed no signs of damage or cell death. The stability and possible trans-esterification of DABO is shortly discussed. Chemical calculations and quantitative structure-activity relationships (QSAR) analysis of DABO and the BNCT agent BPA indicated that they should be cell permeant and accumulate within lysosomes and melanosomes. Molecular modeling allows visualization of both the DABO precursor and the structure of a borate derivative of the proposed catechol-porphycene model for eumelanin, showing interesting features from molecular orbital calculations. The main difference between DABO and other agents, such as BPA, is that it is not a boronic acid nor a boron cluster. This simple catechol-borate ester (protected from oxidation and blackening) could be administrated to living cells and organisms, in which biosynthesis of boron-melanin in melanoma melanocytes can lead to improved BNCT.

Introduction

The ^{10}boron neutron-capture therapy (BNCT) of cancer has attracted increasing biomedical interest (Feakes, 2001; Wittig *et al.*, 2008a; Barth, 2009; Hopewell *et al.*, 2011; Schwint and Trivillin, 2015; Farhood *et al.*, 2018; Fukuda, 2021; Sauerwein *et al.*, 2021). According to the nuclear equation: $^{10}B + {}^{1}n \rightarrow {}^{4}He + {}^{7}Li + \gamma$, the process requires a stable ^{10}B-containing agent that accumulates selectively in the tumor, which is then irradiated with slow, low-energy thermal neutrons. After neutron capture by the ^{10}B isotope, a nuclear fission occurs, which generates extremely fast-moving ^{4}He (α particle), ^{7}Li, and γ radiation from the excited ^{7}Li nucleus (Hopewell *et al.*, 2011; Hu *et al.*, 2020).

The reaction $^{10}B(n, \alpha, \gamma)^{7}Li$ damages tumor cells locally because of the very short braking distance (~10 and ~5 μm) of the emitted α particles and recoiling ^{7}Li nuclei in condensed matter, respectively (Wittig *et al.*, 2008a). The content of B in tumor tissue must be high enough (around 10^{9} ^{10}B atoms/cell) to allow for enough capture reactions to occur for confined cell lethality (Schwint and Trivillin, 2015; Hu *et al.*, 2020). Likewise, ^{10}B atoms must also localize close to a therapeutically useful target (e.g., DNA) to be damaged by the energetic α and ^{7}Li particles action. A very desirable advantage of BNCT is that it can also treat undetectable tumor metastases (Pozzi *et al.*, 2012).

*Address correspondence to: Juan C. Stockert, jcstockert@institutoroffo.uba.ar
†Dedicated to Pedro del Castillo Escassi, *in memoriam*
Received: 17 September 2022; Accepted: 26 December 2022

Doi: 10.32604/biocell.2023.026631

The most employed ^{10}B-containing agents, and the only ones approved for use in humans, are 4-borono-phenylalanine (BPA), and the boron clusters decahydro-decaborate (GB-10) and $[Na_2B_{12}H_{11}SH]^{2-}$ (BSH) (Feakes, 2001; Schwint and Trivillin, 2015; Schwint *et al.*, 2020; Sauerwein *et al.*, 2021). As natural boron contains ~81% of ^{11}B and only ~19% of ^{10}B, boron-containing agents must be enriched in ^{10}B to >98% for BNCT (Pozzi *et al.*, 2012). The chemistry of boron-containing metabolites, boron clusters, and carboranes has been reviewed (Kabalka and Yao, 2006; Pietrangeli *et al.*, 2013; Hu *et al.*, 2020), and they are currently applied for BNCT of skin melanomas (Mishima *et al.*, 1989; Fukuda *et al.*, 1999; González *et al.*, 2004; Menéndez *et al.*, 2009; Carpano *et al.*, 2015; Hiratsuka *et al.*, 2020).

BPA is an amino acid derivative and not a catechol, and therefore it would be highly unlikely to be of use as a specific melanin precursor. Melanoma response to BPA have been proposed to be due to the formation of a complex with l-3,4-dihydroxyphenylalanine (DOPA), dihydroxy-indole (DHI), and 5,6-dihydroxyindole-2-carboxylic acid (DHICA) monomers and thus it would be incorporated into melanin (Yoshino *et al.*, 1997; Fukuda, 2021). Alternatively, as a catechol-reactive reagent (Yan *et al.*, 2005), BPA could form directly specific esters with already formed eumelanin, working as a melanin-reactive drug (Stockert, 2022), namely a melanoma seeker (Stockert *et al.*, 2022) and not as a melanin precursor. This is an expected feature that seems to have been overlooked. Nonetheless, BPA is also taken up by any kind of cancer cells because of enhanced amino acid transport displayed by proliferating cells. In an early approach to carry ^{10}B into melanoma cells using 3,4-dihydroxy-L-phenylalanine (L-DOPA) as a melanin catechol-containing precursor, DOPA-borate was synthesized (Yoshino *et al.*, 1979) but no further results have been reported regarding the application of this compound.

On the other hand, several reviews have been published on melanin structure and biosynthesis (d'Ischia *et al.*, 2015; Scognamiglio *et al.*, 2017; Blázquez-Castro and Stockert, 2021; Stockert and Blázquez-Castro, 2022). The first melanin precursor is L-tyrosine (Fig. 1A), which is converted to L-DOPA by tyrosinase, and to dopamine (DA) by decarboxylation, yielding the synthetic eumelanin-like poly-DA (PDA) by spontaneous oxidative polymerization (Dreyer *et al.*, 2012; Micillo *et al.*, 2016). PDA now has numerous biotechnological applications (Hauser *et al.*, 2020; Liu *et al.*, 2020). In the presence of the borate anion (BO), DA should generate the dopamine-borate complex (DABO, Fig. 1B), which can form dihydroxy-indole (DHI)-borate (DHIBO) (Fig. 1C), and then the corresponding borate derivative of the proposed eumelanin model, poly-catechol-porphycene (poly-CPo) (Stockert, 2021; Stockert and Blázquez-Castro, 2022).

Considering the great number of catechol groups in eumelanin (di Mauro *et al.*, 2017; Ruiz-Molina *et al.*, 2018; Cavallini *et al.*, 2020) and that each precursor molecule has a catechol that can complex with borate anion, numerous borate esters could be introduced into eumelanin. The binding of metal ions can account for up to 6×10^{20} sites per gram of dried melanin (Sarna *et al.*, 1976), and therefore

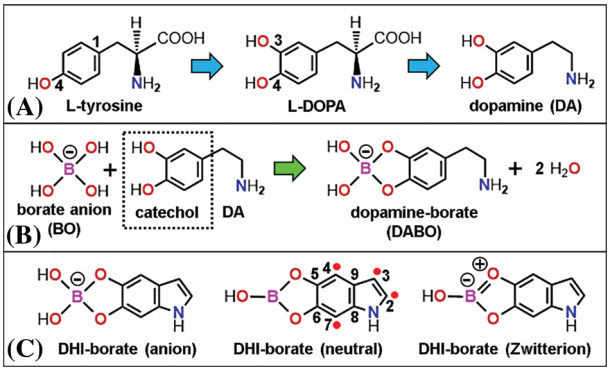

FIGURE 1. Chemical structure (with atom numbering) of (A) eumelanin precursors: L-tyrosine, L-DOPA, and dopamine (DA), (B) reagents: borate anion (BO), DA and product: dopamine-borate complex (DABO), and (C) dihydroxy-indole (DHI)-borate, shown as a tetrahedral anion, trigonal neutral form, and Zwitterion. In this case, the amphiphilic BO ring exhibits 6π-electron resonance (Gerrard *et al.*, 1959). Blue and green arrows indicate precursor oxidation and formation of the BO ester, respectively. Red circles show the carbon radicals allowing DHI polymerization (Stockert and Blázquez-Castro, 2022).

in the case of PDA, after excluding N binding sites, the remaining O sites are catechols, which would account for a considerable amount of melanin-bound B atoms.

Catechols, flavonols, anthraquinones, β-diketones, etc., are known to give stable borate complexes (Frohne, 1974; Yoshino *et al.*, 1979; Yang *et al.*, 2003; Lenskiy *et al.*, 2020). Borax is widely used as a cross-linking agent between hydroxyl groups (Frasconi *et al.*, 2009), and fluorescent boronic acid (C-B[OH]$_2$) derivatives are applied for the detection of specific carbohydrates by forming stable borate-*cis* diol 1:1 esters with mannose, gulose, allose, talose, rhamnose, ribose, etc. (Gallop *et al.*, 1982, Yang *et al.*, 2003; Yan *et al.*, 2005; Stockert and Blázquez-Castro, 2017). Once borate anions are formed at alkaline pH (higher than ~8), they lose the hydroxyls at acid pH (lower than ~7) or in non-aqueous media and become neutral (non-ionized) trigonal borate (BO_3) esters (Yoshino *et al.*, 1979; Yang *et al.*, 2003; Yan *et al.*, 2005).

The melanin precursor DA is a neurotransmitter involved in neurological diseases and used for cardiac stimulation, shock-states therapy, and dietary supplement. Considering a previous proposal of using a DOPA-borate complex for BNCT (Yoshino *et al.*, 1979), we have performed a preliminary study to substantiate the use of a similar DABO agent as a ^{10}B carrier for BNCT. As far as we know, this is the first report of both formation of a catechol-borate derivative of the melanin precursor DA and its autopolymerization into the soluble melanin-like poly-dopamine-borate (PDABO) product, resulting in a simple way to attach boron to a melanin precursor.

Materials and Methods

Dopamine hydrochloride (DA, 189.6 g/mol), and disodium tetraborate decahydrate (borax, 381.4 g/mol) (both from Sigma-Aldrich), were used as purchased. Synthesis of the 1:1 dopamine-borate (DABO) complex was performed

according to the published method using L-DOPA (Yoshino *et al.*, 1979). First, 0.381 g of borax was dissolved in 100 mL of deionized water, and then 0.189 g of DA was slowly added until total dissolution, thus obtaining a concentration of 10 mM for each component and a pH of 9. In borax and boric acid solutions at pH values higher than 8, the monomeric borate anion ($B[OH]_4^-$) is the unique borate (BO) compound (Yoshino *et al.*, 1979). The solution was maintained at room lightening and temperature (about 22°C) and allowed to spontaneously oxidize for 24 h.

In some samples, after mixing DA and BO, ascorbic acid (0.5 mg/mL) was added to the still colorless DABO product, and the pH was adjusted to 7 with 5 % acetic acid. This product was then stored in an airtight container and frozen in the darkness for 50 days. Other DABO samples were lyophilized, diluted in H_2O at pH 9, and exposed for several days to air and light for auto-polymerization. Because of the low water solubility of borax, boric acid (61.8 g/mol) at pH 9 could also be used as a 10 mM solution to form the DABO product.

Cultured OL living cells from an oral canine melanotic melanoma (Rossi *et al.*, 2015) (kindly provided by L.M.E. Finocchiaro and G.C. Glikin) grown to confluence in complete DMEM medium were treated with DABO (1 mM in complete DMEM for 24 and 48 h), washed and mounted in phosphate-buffered saline, and observed under phase contrast microscopy. Cytochemical attempts to reveal boron in DABO-treated cells using morin- and benzoin-induced fluorescence with borate groups (Udenfriend, 1962; Feigl and Anger, 1972; Frohne, 1974) under 436 and 365 nm excitation, respectively, were also carried out.

X-ray microanalysis (XRMA) of PDA and PDABO samples was performed using a field-emission scanning electron microscope (Zeiss GeminiSEM 500), equipped with energy dispersive X-ray device (Oxford Instruments, UltimExtreme detector, and AZtec software), working at 2 kV and 5 mm distance. Before XRMA, dried samples were washed with 5% acetic acid for 30 min to remove unbound borate ions. Samples of OL melanoma cells without treatment or treated with 1 mM DABO for 24 and 48 h were also subjected to XRMA for the detection of B.

On the other hand, to analyze theoretical possibilities for DABO uptake and organelle localization in living cells, quantitative structure-activity relationships (QSAR) parameters of DABO and the boronic agent BPA were inspected according to the well-known prediction rules and flow charts (Horobin *et al.*, 2013; Horobin *et al.*, 2015; Stockert and Blázquez-Castro, 2017; Horobin *et al.*, 2021). Used QSAR parameters available in the HyperChem v8.0.10 software were nominal electric charge (Z), molecular weight (mass), and hydrophilicity-lipophilicity (logarithm of the water-octanol partition coefficient, log P). The conjugated bond number (CBN) was calculated by inspecting and recording conjugated bonds. Acid-base strength (pK_a) values were taken from https://pubchem.ncbi.nlm.nih.gov.

Molecular modeling studies (e.g., Stockert *et al.*, 2022; Stockert and Felix-Pozzi, 2023) illustrating the comparative structure of DABO and BPA, as well as the molecular orbitals of DABO, DHI-borate (DHIBO), and a tetra-CPo-borate model of eumelanin were also performed using the HyperChem v7 software, and MM+ geometry optimization converged at energy E = 0.1, 0.05, and 0.01 kcal/(Å mol). Energy minimization was calculated using the semi-empirical parametric method 3 (PM3) method (Polak-Riviere conjugate gradient) converged at E = 0.05 kcal/(Å mol) or the extended-Hückel method.

Results and Discussion

After 24 h exposure to air and light, the aspect of 5 mL DA and DABO solutions shows their typical blackening by polymerization to yield PDA and its borate complex (PDABO) (Figs. 2B and 2C), as well as non-blackening of the unoxidized DABO precursor (Figs. 2A and 2D), and blackening of a previously lyophilized DABO solution (Fig. 2E). The presence of boron only in PDABO is confirmed by comparing XRMA spectra (Figs. 2F and 2G), which clearly show the peak of B at 0.183 keV.

Obviously, although spontaneous polymerization of DABO *in vitro* confirms its capacity to serve as melanin precursor *in vivo*, the DABO product needs to be protected from oxidation and polymerization before its use in living cells and organisms. This requisite was checked in fresh samples kept with ascorbic acid, frozen in darkness without air, yielding a transparent DABO solution after thawing that blackened over time. Likewise, frozen DABO subjected to lyophilization and dissolved in water also blackened (Fig. 2E). The autocatalytic assembly of the polymer can be assumed to occur through radicals formed at the C2, C3, C4, and C7 positions in the DHI precursor (Stockert and Blázquez-Castro, 2022) (Fig. 1C). Interestingly, the presence of 5,6-borate esters in DHI units does not prevent the autopolymerization and blackening of DABO solutions. The 2-carboxyl group (missing in DA) is also not essential for autopolymerization (d'Ischia *et al.*, 2015).

To analyze the possible microscopical effects of DABO, the morphology of living cultures of melanoma OL melanocytes was studied (Fig. 3). After 1 mM DABO treatment for 24 and 48 h, the characteristic shape of OL cells was observed, showing clearly normal features and no signs of cell damage or death (Fig. 3). Thus, it is logical to assume that the DABO analog is non-toxic to OL cells, which grow continuously reaching confluence and forming 3D networks. Similarities of BPA and DABO with the amino acid and catecholamine metabolites, respectively, explain the absence of cell toxicity at a millimolar concentration, which contrasts with the toxicity of antitumoral drugs (e.g., most photodynamic agents at 10^{-5} M or higher concentration (Villanueva *et al.*, 2003; Stockert *et al.*, 2004; Cañete *et al.*, 2009)).

Unfortunately, the occurrence of boron in DABO-treated cells could not be recorded by XRMA because the sensitivity of the equipment was not enough to reveal the B peak in single melanocytes. Likewise, cytochemical attempts to reveal B by using morin and benzoin methods under fluorescence microscopy were also unsuccessful, likely due to their sensitivity limit to detect B within melanosomes.

However, comparative analysis of molecular structure and properties between the precursors DA and phenylalanine (PA), with the corresponding boron-

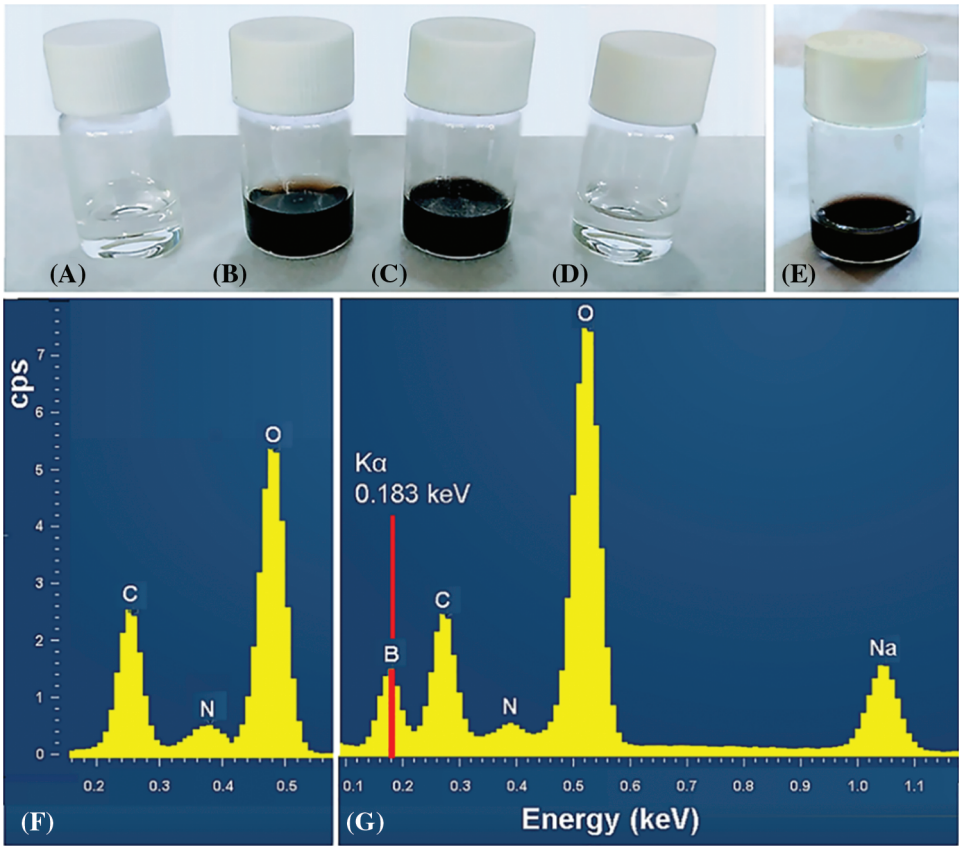

FIGURE 2. (A, B): Aspect of a 10 mM DA solution, immediately prepared (A) and 24 h later, exposed to air and light (B). (C, D): Aspect of 10 mM DABO solutions, exposed to air and light for 24 h (C), and a DABO solution after addition of ascorbic acid (0.5 mg/mL), stored airtight and frozen in darkness for 50 days (D). (E): Blackening of a lyophilized DABO sample diluted in H_2O at pH 9 and exposed to air and light for 72 h. (F, G): X-ray microanalysis of dried poly-DA (F) and poly-DA-borate complex (G) samples showing the boron signal (red line) and peaks of other elements (cps: counts per second).

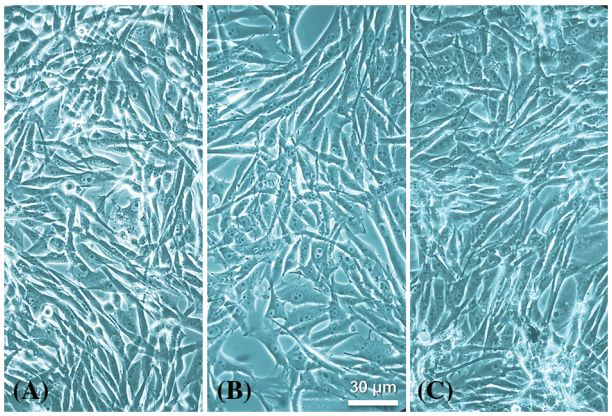

FIGURE 3. Cultured OL melanotic cell line observed under phase contrast. (A) Control (untreated) cells. (B and C) OL cells treated with 1 mM DABO for 24 h (B) and 48 h (C). Treated living melanoma cells are clearly undamaged and show a fusiform or dendritic shape, with light nuclei, compact nucleoli and dark round and ovoid melanosomes in the cytoplasm. Melanin-containing dense endings of cytoplasm prolongations are also observed.

containing analog agents DABO and the well-known BPA showed interesting and clear similarities, which support a similar behavior in relation to cell uptake. Both DABO and BPA have analogous sizes and shapes, as well as a similar distribution of electrostatic potentials (Fig. 4).

Considering that BPA enters and accumulates into live cells (Chandra *et al.*, 2002; Wittig *et al.*, 2008b; Chandra *et al.*, 2008), it is conceivable that the analogous agent DABO is also a permeant metabolite derivative. In addition to their general resemblance, QSAR parameters of DABO and BPA have the same range of values (Table 1), indicating that both agents enter live cells easily. A likely accumulation of these agents in lysosomes and related structures such as melanosomes (with a clear lysosomal lineage (Orlow, 1995; Raposo and Marks, 2007)) can be predicted according QSAR rules for acidophilic weak bases, which requires agreement with the following parameters: $Z_{nominal} \geq 0$; CBN < 40; log $P_{cation} < 0$ and log $P_{uncharged} > 0$; $10 > pK_a > 6$ (Rashid *et al.*, 1991; Horobin *et al.*, 2013; Stockert and Blázquez-Castro, 2017). Therefore, it is tempting to assume that after cell uptake, both DABO and BPA should be localized within lysosomes and melanosomes according to their predictive QSAR values (see Table 1).

A few papers have been devoted to the localization of B-containing drugs for BNCT, but they have shown rather poor results. ^{18}F-BPA was found in cytoplasm and nuclei of human glioblastoma and murine sarcoma cells (Chandra *et al.*, 2002; Wittig *et al.*, 2008b; Chandra *et al.*, 2008). In contrast, BSH-containing amino acids appeared localized in perinuclear granules after BSH immuno-staining of glioma cells (Hattori *et al.*, 2012). In the case of melanocytes, DABO appears as a suitable boronated precursor of eumelanin biosynthesis and thus it should be accumulated specifically in melanosomes and considered for BNCT. In this context, melanosomes are known to be lysosome-like acidic organelles, with an intramelanosomal pH range as low as 3–5, due to the activity of a proton-translocating ATPase (Orlow, 1995; Raposo and Marks, 2007). This physiological feature accounts for the likely occurrence of non-ionized borate esters of eumelanin within melanosomes.

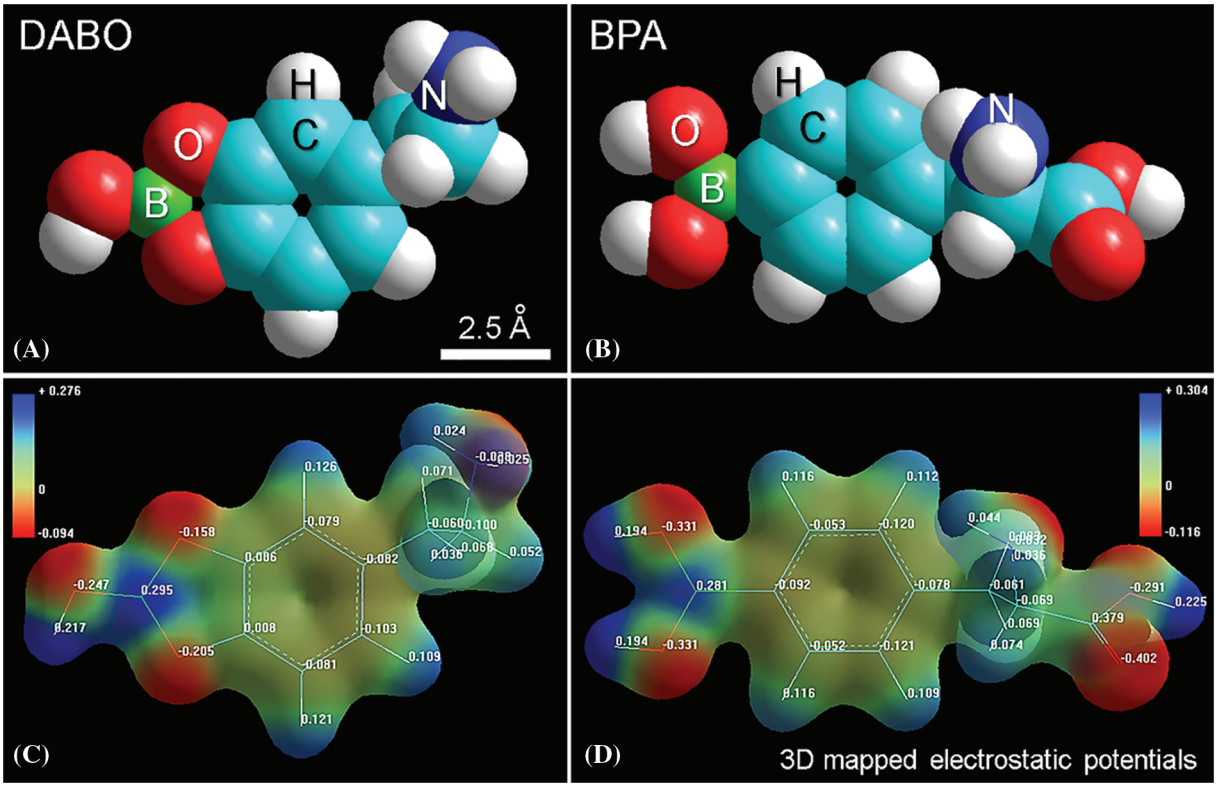

FIGURE 4. (A, B) Atomic volume models of DABO and BPA, respectively, showing their similar molecular morphology. (C, D) Isosurface 3D mapped electrostatic potentials of DABO and BPA showing a similar distribution of differential positive and negative charges.

TABLE 1

QSAR parameters of precursors and analogs mentioned in this work, which support their localization in lysosomes and melanosomes

Precursors or analogs[a]	Z[b]	CBN[c]	Log P[d]	MW[e]	pKa[f]
DA	0	6	+0.85	153.18	8.93
DABO	0	6	+0.88	178.98	na
PA	0	6	+1.42	165,19	9.12
BPA	0	6	+1.03	209.01	na

Note: a: uncharged trigonal boron in DABO and BPA; b: nominal electric charge; c: number of conjugated (resonant) double bonds; d: only approximate values because no parameter is available in the software for B atom; e: values without counterions; f: na, no available values.

Considering the well-known stereochemical aspects of the formation of catechol-borate esters (Gerrard *et al.*, 1959; Lang *et al.*, 1997; Yan *et al.*, 2005; Lenskiy *et al.*, 2020) and the use of molecular modeling methods in studies on the chemistry of eumelanin (Stockert and Blázquez-Castro, 2022; Stockert *et al.*, 2022; Stockert and Felix-Pozzi, 2023), the DABO and DHIBO precursors, as well as the catechol-porphycene proposed for eumelanin were modeled. The characteristic trigonal configuration of neutral borate group in the catechol-5,6-borate ester was found in both DABO and DHIBO models, in agreement with geometric features of boric acid and its neutral esters (Gerrard *et al.*, 1959; Yoshino *et al.*, 1979; Lang *et al.*, 1997; Schubert *et al.*, 2003; Tsuyumoto *et al.*, 2007). This trigonal π-electron conjugation of the O-B-O bonds is illustrated in the case of DHIBO (Fig. 5).

The relation between pH, ionization and geometry of the borate group is well known, but the stabilizing π-electron resonance between O and B atoms of the borate ester in the zwitterionic mesomers of DHIBO appears rather overlocked. Interestingly, molecular modeling shows a clear π-conjugation involving the O-B-O atoms of the borate ring (Fig. 5).

Regarding stability, it is accepted that the kinetics of borate ester formation with catechols from borates and boronic acid *in vitro* allows a rapid and effective synthesis of the corresponding catechol-borate complexes (Yasunobu and Norris, 1957; Roy and Brown, 2007; Tsuyumoto *et al.*, 2007, Bernardini *et al.*, 2009; Ketuly and Hadi, 2010; Pereira Silva *et al.*, 2020). It is commonly accepted that borate esters of aliphatic *cis*-diols, catechols and substituted catechols with borates or boronic acids are reasonably stable under non-dramatic hydrolytic conditions, mainly those from catechols (Roy and Brown, 2007; Bernardini *et al.*, 2009; Ketuly and Hadi, 2010).

Accordingly, borate-catechol esters are stable enough regarding hydrolysis and trans-esterification under physiological conditions. Therefore, borate trans-esterification, if any, would result in the formation of another borate ester from a previously established one, overall resulting in the same end result. If boron atoms remain within cells, trans-esterification is not relevant, because only boron atoms are needed for BNCT.

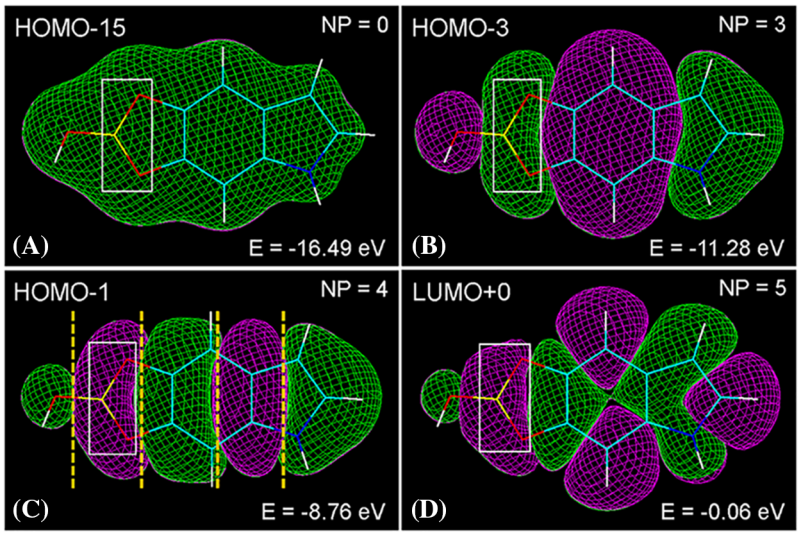

FIGURE 5. (A–D) Wire molecular models (C: cyan, O: red, N: blue, H: white, B: yellow) of the eumelanin precursor 5,6-dihydroxy-indole-borate (DHIBO, neutral form) in frontal view, showing different HOMO and LUMO energy levels with positive (green) and negative (violet) molecular orbitals. Rectangles indicate the O-B-O bonds from the catechol-borate ester showing π-electron conjugation. Nodal planes (NP, dashed yellow lines in HOMO-1) separate green and violet orbital lobes, high energy levels corresponding to high number of nodal planes (Stockert and Blázquez-Castro, 2017). PM3 energy minimization (Polak-Ribiere) converged at energy E = 0.05 kcal/(Å mol), and Jorgensen-Salem surface rendering with orbital contour: 0.003.

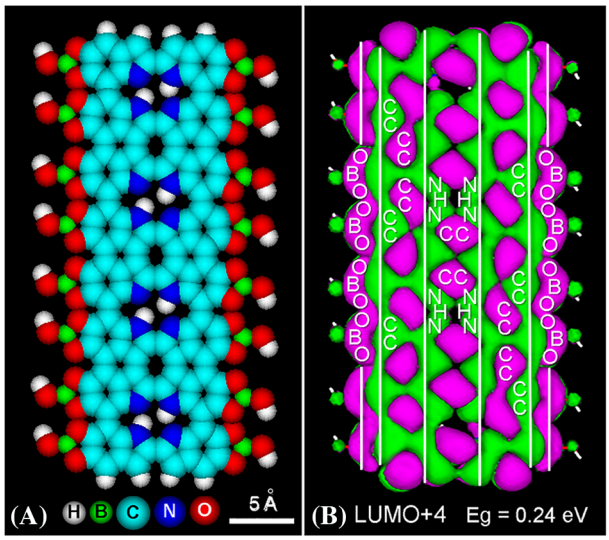

FIGURE 6. Structure of tetra-CPo modeled with DABO precursors. (A): Frontal atomic volume of the tetra-CPo model with DHIBO units located along the free external edges, after geometry optimization with MM+ converged at E = 0.01 kcal/(Å mol). Note the trigonal borates and the planar structure of the oligomer. N: HN bonding distances are 2.7–2.8 Å. (B): LUMO+4 energy level (−9.83 eV) using the extended Hückel energy minimization (864 orbitals), Gouraud shaded 3D isosurface, orbital contour: 0.0002, and Eg = 0.24 eV. Observe the extended longitudinal LUMO+4 lobes corresponding to the π*-electron conjugated CC and N:HN atoms (vertical white lines), as well as the contiguous pairs of conjugated borate groups (O-B-O).

Anyway, boric acid that could result from any hydrolytic process is a Lewis' acid that interacts with water giving tetrahydroxy-borate anions ($B[OH]_4^-$, pKa = 9.24), and poly-borate anions at pH ≥ 7 (Jolly, 1984; Tsuyumoto *et al.*, 2007). Therefore, possible borate anions released from catechol esters are slightly acid xenobiotics with low elimination rate from living organism (Harvey, 1980; EPA, 1993). This feature should damage living cells, but however, no toxicity is found after DABO treatment of cultured OL melanocytes for 24–48 h (Fig. 3).

Even in the case that B-containing compounds could result from intracellular (likely lysosomal) degradation of the DABO precursor or newly formed DABO polymer, it can be assumed that B atoms still remain available for BNCT, and this is the most relevant concept. Regarding lysosomes, they finally become multivesicular or residual bodies (often containing lipofuscins and myelin figures) when their contents are indigestible materials, and they are not generally extruded to the outside but normally remain indefinitely within cells (Pitt, 1975). The fate of possible degradation products from boron compounds would be the same as colloidal metals, metal oxides, carbon, polymeric nanoparticles, vital dyes and fluorescent probes, which are selectively accumulated within lysosomes and melanosomes (Allison, 1968; Rashid *et al.*, 1991; Horobin, 2010; Stockert *et al.*, 2022).

Regarding the proposed poly-CPo model, it must be noted it fulfills all characteristic features of natural and synthetic eumelanin such as high double-bond conjugation, broad-band light absorption, as well as X-ray crystallography and electron microscopy results (Stockert and Blázquez-Castro, 2022; Stockert *et al.*, 2022), appearing the polymers as a multilayer graphitic structure. Modeling of a planar tetra-CPo molecule containing DHIBO units illustrates the organization of the final complex, namely the possible tetra-CPo-borate eumelanin model (Fig. 6). Long continuous LUMO+4 lobes showing trigonal O-B-O groups, and fused C=C and N:HN orbitals are clearly visible, accounting for the massive aromatic conjugation and reduction of the Eg in this graphitic material.

It is interesting to remark that borate binding to O5 and O6 catechol sites in DHIBO does not hinder the autopolymerization of DABO but prevents the formation of ether bridges, polymer curvature, and the spiral organization of poly-CPo (Stockert *et al.*, 2022; Stockert and Blázquez-Castro, 2022; Stockert and Felix-Pozzi, 2023). No curvature is also found in the case of borate esters either in the 5,5′ or 6,6′ position. Anyway, as catechol groups are present in simpler eumelanin structures (d'Ischia *et al.*, 2015; Micillo *et al.*, 2016; Blázquez-Castro and Stockert, 2021), they could also account for the occurrence of borate esters introduced as DABO precursors in other eumelanin models.

Perspectives and Conclusions

In addition to DABO, other melanin precursors could incorporate borate and be used as ^{10}B-containing agents. Thus, borate esters formed with the catechol group of norepinephrine and DHI could be applied for BNCT. Likewise, an interesting metabolite analog of DHI would be the new compound catechol-imidazole, which is able to form a catechol-imidacene (CIm) polymer (Stockert and Felix-Pozzi, 2023). The borate ester CImBO should also be a melanin precursor and a potential ^{10}B-carrier candidate for BNCT. All the possible catechol-borate precursors could be not only incorporated during eumelanin biosynthesis, but they would also be suitable for direct binding to the catechol groups of already formed polymers (Stockert, 2022), like specific melanin-seeker agents.

In this study, we demonstrate that DABO spontaneously oxidizes and autopolymerizes *in vitro*, giving a soluble and stable eumelanin-like brown-black PDABO product. The main difference between DABO and other boron-containing agents (BPA, MSH, etc.) is that it is not a boronic acid nor a boron cluster but a simple catechol-borate ester. After administration of the DABO precursor (protected from oxidation and blackening) into living cells and organisms, enzymatic biosynthesis of boron-melanin in melanoma melanocytes is envisioned to lead to improved BNCT.

Acknowledgement: We thank JL Bella, MM Blanco, J Espada, LL Colombo, A Koss, MJ Planes Insausti, GR Solarz, A Stockert, and A Urtreger for valuable collaboration and stimulating discussions.

Funding Statement: These authors received no specific funding for this study.

Author Contributions: The authors confirm contribution to the paper as follows: study conception and design: JC Stockert; experimental work: SA Romero, MN Felix-Pozzi; manuscript preparation, edition and formatting: JC Stockert, A Blázquez-Castro. The authors reviewed the results and approved the final version of the manuscript.

Availability of Data and Materials: All data generated or analyzed during this study are included in this published article.

Ethics Approval: Not applicable.

Conflicts of Interest: The authors declare that they have no conflicts of interest to report regarding the present study.

References

Allison AC (1968). Effects of drugs and toxic agents on lysosomes. In: Campbell PN (ed.), *Interaction of Drugs and Subcellular Compartments in Animal Cells,* pp. 218–236. London: J. & A. Churchill Ltd.

Barth RF (2009). Boron neutron capture therapy at the crossroads: Challenges and opportunities. *Applied Radiation and Isotopes* **67**: 3–6. https://doi.org/10.1016/j.apradiso.2009.03.102

Bernardini R, Oliva A, Paganelli A, Menta E, Grugni M, de Munari S, Goldoni L (2009). Stability of boronic esters to hydrolysis: A comparative study. *Chemistry Letters* **38**: 750–751. https://doi.org/10.1246/cl.2009.750

Blázquez-Castro A, Stockert JC (2021). Biomedical overview of melanin. 1. Updating melanin biology and chemistry, physico-chemical properties, melanoma tumors, and photothermal therapy. *BIOCELL* **45**: 849–862. https://doi.org/10.32604/biocell.2021.015900

Carpano M, Perona M, Rodriguez C, Nievas S, Olivera M et al. (2015). Experimental studies of boronophenylalanine ((10) BPA) biodistribution for the individual application of boron neutron capture therapy (BNCT) for malignant melanoma treatment. *International Journal of Radiation Oncology, Biology, Physics* **93**: 344–352. https://doi.org/10.1016/j.ijrobp.2015.05.039

Cavallini C, Vitiello G, Adinolfi B, Silvestri B, Armanetti P, Manini P, Pezzella A, d'Ischia M, Luciani G, Menichetti L (2020). Melanin and melanin-like hybrid materials in regenerative medicine. *Nanomaterials* **10**: 1518. https://doi.org/10.3390/nano10081518

Cañete M, Stockert JC, Villanueva A (2009). Preclinical photodynamic therapy research in Spain. 3. Localization of photosensitizers and mechanisms of cell death *in vitro*. *Journal of Porphyrins and Phthalocyanines* **13**: 544–551. https://doi.org/10.1142/S1088424609000516

Chandra S, Kabalka GW, Lorey DR, Smith DR, Coderre JA (2002). Imaging of fluorine and boron from fluorinated boronophenylalanine in the same cell at organelle resolution by correlative ion microscopy and confocal laser scanning microscopy. *Clinical Cancer Research* **8**: 2675–2683. PMID 12171900.

Chandra S, Tjarks W, Lorey DR, Barth RF (2008). Quantitative subcellular imaging of boron compounds in individual mitotic and interphase human glioblastoma cells with imaging secondary ion mass spectrometry (SIMS). *Journal of Microscopy* **229**: 92–103. https://doi.org/10.1111/j.1365-2818.2007.01869.x

di Mauro E, Xu R, Soliveri G, Santato C (2017). Natural melanin pigments and their interfaces with metal ions and oxides: Emerging concepts and technologies. *MRS Communications* **7**: 141–151. https://doi.org/10.1557/mrc.2017.33

Dreyer DR, Miller DJ, Freeman BD, Paul DR, Bielawski CW (2012). Elucidating the structure of poly(dopamine). *Langmuir* **28**: 6428–6435. https://doi.org/10.1021/la204831b

d'Ischia M, Wakamatsu K, Cicoira F, di Mauro E, Garcia-Borron JC, Commo S (2015). Melanins and melanogenesis: From

pigment cells to human health and technological applications. *Pigment Cell and Melanoma Research* **28**: 520–544. https://doi.org/10.1111/pcmr.12393

EPA (1993). *R.E.D. Facts: Boric acid.* United States Environmental Protection Agency. Office of Prevention, Pesticides and Toxic Substances (7508W) EPA-738-F-93-006.

Farhood B, Samadian H, Ghorbanic M, Zakariaeed SS, Knaup C (2018). Physical, dosimetric and clinical aspects and delivery systems in neutron capture therapy. *Reports of Practical Oncology and Radiotherapy* **23**: 462–473. https://doi.org/10.1016/j.rpor.2018.07.002

Feakes DA (2001). Chemistry and pharmacology of agents for BNCT. In: Hawthorne MF, Shelley K, Wiersema RJ (eds.), *Frontiers in Neutron Capture Therapy,* vol 1, pp. 23–34. Boston, MA: Springer.

Feigl F, Anger V (1972). *Spot Tests in Inorganic Analysis.* 6th edition, pp. 136–142. Amsterdam: Elsevier Publishing Co.

Frasconi M, Rea S, Matricardi P, Favero G, Mazzei F (2009). Scleroglucan-borax hydrogel: A flexible tool for redox protein immobilization. *Langmuir* **25**: 11097–11104. https://doi.org/10.1021/la901245z

Frohne D (1974). *Anatomisch-mikrochemische Drogenanalyse.* Stuttgart: Georg Thieme Verlag.

Fukuda H (2021). Boron neutron capture therapy (BNCT) for cutaneous malignant melanoma using 10B-p-boronophenylalanine (BPA) with special reference to the radiobiological basis and clinical results. *Cells* **10**: 2881. https://doi.org/10.3390/cells10112881

Fukuda H, Honda C, Wadabayashi N, Kobayashi T, Yoshino K et al. (1999). Pharmacokinetics of 10B-p-boronophenylalanine in tumors, skin and blood of melanoma patients: A study of boron neutron capture therapy for malignant melanoma. *Melanoma Research* **9**: 75–83. https://doi.org/10.1097/00008390-199902000-00010

Gallop PM, Paz MA, Henson E (1982). Boradeption: A new procedure for transferring water-insoluble agents across cell membranes. *Science* **217**: 166–169. https://doi.org/10.1126/science.6178158

Gerrard W, Lappert MF, Mountfield BA (1959). Interaction of boron trichloride with catechol, quinol, resorcinol, and pyrogallol. *Journal of the Chemical Society*: 1529–1535. https://doi.org/10.1039/jr9590001529

González SJ, Bonomi MR, Santa Cruz GA, Blaumann HR, Calzetta Larrieua OA et al. (2004). First BNCT treatment of a skin melanoma in Argentina: Dosimetric analysis and clinical outcome. *Applied Radiation and Isotopes* **61**: 1101–1105. https://doi.org/10.1016/j.apradiso.2004.05.060

Harvey C (1980). Antiseptics and disinfectants; Fungicides; Ectoparasites. In: Gilman AG, Godman LS, Gilman A, (eds.), *The Pharmacological Basis of Therapeutics.* 6th edition. New York: Macmillan.

Hattori Y, Kusaka S, Mukumoto M, Uehara K, Asano T, Suzuki M, Masunaga S, Ono K, Tanimori S, Kirihata M (2012). Biological evaluation of dodecaborate-containing L-amino acids for boron neutron capture therapy. *Journal of Medicinal Chemistry* **55**: 6980–6984. https://doi.org/10.1021/jm300749q

Hauser D, Septiadi D, Turner J, Petri-Fink A, Rothen-Rutishauser B (2020). From bioinspired glue to medicine: Polydopamine as a biomedical material. *Materials* **13**: 1730. https://doi.org/10.3390/ma13071730

Hiratsuka J, Kamitani N, Tanaka R, Tokiya R, Yoden E, Sakurai Y, Suzuki M (2020). Long-term outcome of cutaneous melanoma patients treated with boron neutron capture therapy (BNCT). *Journal of Radiation Research* **61**: 945–951. https://doi.org/10.1093/jrr/rraa068

Hopewell JW, Morris GM, Schwint A, Coderre JA (2011). The radiobiological principles of boron neutron capture therapy: A critical review. *Applied Radiation and Isotopes* **69**: 1756–1759. https://doi.org/10.1016/j.apradiso.2011.04.019

Horobin RW (2010). Can QSAR models describing small-molecule xenobiotics give useful tips for predicting uptake and localization of nanoparticles in living cells? And if not, why not?. In: Weissig V, D'Souza GGM, eds. *Organelle-Specific Pharmaceutical Nanotechnology.* New York: Wiley, 193–206.

Horobin RW, Stockert JC, Rashid-Doubell F (2013). Uptake and localisation of small-molecule fluorescent probes in living cells: A critical appraisal of QSAR models and a case study concerning probes for DNA and RNA. *Histochemistry and Cell Biology* **139**: 623–637. https://doi.org/10.1007/s00418-013-1090-0

Horobin RW, Stockert JC, Rashid-Doubell F (2015). Uptake and localization mechanisms of fluorescent and colored lipid probes. Part 2. QSAR models predicting localization of fluorescent probes used to identify (specifically stain) various biomembranes and membranous organelles. *Biotechnic and Histochemistry* **90**: 241–254. https://doi.org/10.3109/10520295.2015.1005129

Horobin RW, Stockert JC, Zhang H (2021). Reactive dyes for living cells—Applications, artefacts, and some comparisons with textile dyeing. *Coloration Technology.* https://doi.org/10.1111/cote.12577

Hu K, Yang Z, Zhang L, Xie L, Wang L, Xu H, Josephson L, Liang SH, Zhang MR (2020). Boron agents for neutron capture therapy. *Coordination Chemistry Reviews* **405**: 213139. https://doi.org/10.1016/j.ccr.2019.213139

Jolly W (1984). *Modern Inorganic Chemistry.* New York: McGraw-Hill.

Kabalka GW, Yao ML (2006). The synthesis and use of boronated amino acids for boron neutron capture therapy. *Anti-Cancer Agents in Medicine and Chemistry* **6**: 111–125. https://doi.org/10.2174/187152006776119144

Ketuly KA, Hadi AHA (2010). Boronate derivatives of functionally diverse catechols: Stability studies. *Molecules* **15**: 2347–2356. https://doi.org/10.3390/molecules15042347

Lang A, Knizek J, Nöth H, Schur S, Thomann M (1997). Beiträge zur Chemie des Bors. 237. Bis(benzo-l,3,2-dioxaborolanyl) oxid und 2-(o-Hydroxyphenoxy)-benzo-l,3,2-dioxaborolan. Vorstufen zur Synthese von Catecholboran (Benzo-l,3,2-dioxaborolan). *Zeitschrift für anorganische und allgemeine Chemie* **623**: 901–907. https://doi.org/10.1002/(ISSN)1521-3749

Lenskiy MA, Shul'ts EE, Korabel'nikov DV, Ozhogin AV, Novitskiy AN (2020). Pyrocatechol borates: Synthesis, reaction with formaldehyde, and solvent effect on polycondensation process. *Polymer* **188**: 122162. https://doi.org/10.1016/j.polymer.2020.122162

Liu H, Yang Y, Liu Y, Pan J, Wang J, Man F, Zhang W, Liu G (2020). Melanin-like nanomaterials for advanced biomedical applications: A versatile platform with extraordinary promise. *Advances in Science* **7**: 1903129. https://doi.org/10.1002/advs.201903129

Menéndez PR, Roth BMC, Pereira MD, Casal MR, González SJ et al. (2009). BNCT for skin melanoma in extremities: Updated

Argentine clinical results. *Applied Radiation and Isotopes* **67**: S50–S53. https://doi.org/10.1016/j.apradiso.2009.03.020

Micillo R, Panzella L, Koike K, Monfrecola G, Napolitano A, D'Ischia M (2016). Fifty shades of black and red or how carboxyl groups fine tune eumelanin and pheomelanin properties. *International Journal of Molecular Sciences* **17**: 746. https://doi.org/10.3390/ijms17050746

Mishima Y, Ichihashi M, Hatta S, Honda C, Yamamura K, Nakagawa T (1989). New thermal neutron capture therapy for malignant melanoma: Melanogenesis-seeking 10B molecule-melanoma cell interaction from *in vitro* to first clinical trial. *Pigment & Cell Research* **2**: 226–234. https://doi.org/10.1111/j.1600-0749.1989.tb00196.x

Orlow SJ (1995). Melanosomes are specialized members of the lysosomal lineage of organelles. *Journal of Investigative Dermatology* **105**: 3–7. https://doi.org/10.1111/1523-1747.ep12312291

Pereira Silva M, Saraiva L, Pinto M, Sousa ME (2020). Boronic acids and their derivatives in medicinal chemistry: Synthesis and biological applications. *Molecules* **25**: 4323. https://doi.org/10.3390/molecules25184323

Pietrangeli D, Rosa A, Ristori S, Salvati A, Altieri S, Ricciardi G (2013). Carboranyl-porphyrazines and derivatives for boron neutron capture therapy: From synthesis to *in vitro* tests. *Coordination Chemistry Review* **257**: 2213–2231. https://doi.org/10.1016/j.ccr.2013.03.035

Pitt D (1975). *Lysosomes and Cell Function*, pp. 12–16+74–77+9–88. London, New York: Longman.

Pozzi ECC, Cardoso JE, Colombo LL, Thorp S, Monti Hughes A et al. (2012). Boron neutron capture therapy (BNCT) for liver metastasis: Therapeutic efficacy in an experimental model. *Radiation and Environment Biophysics* **51**: 331–339. https://doi.org/10.1007/s00411-012-0419-8

Raposo G, Marks MS (2007). Melanosomes—Dark organelles enlighten endosomal membrane transport. *Nature Review Molecular and Cell Biology* **8**: 786–797. https://doi.org/10.1038/nrm2258

Rashid F, Horobin RW, Williams MA (1991). Predicting the behavior and selectivity of fluorescent probes for lysosomes and related structures by means of structure-activity models. *Histochemical Journal* **23**: 450–459. https://doi.org/10.1007/BF01041375

Rossi UA, Gil-Cardeza ML, Villaverde MS, Finocchiaro LME, Glikin GC (2015). Interferon-gene transfer induces a strong cytotoxic bystander effect on melanoma cells. *Biomedicine and Pharmacotherapy* **72**: 44–51. https://doi.org/10.1016/j.biopha.2015.04.002

Roy CD, Brown HC (2007). Stability of boronic esters—Structural effects on the relative rates of transesterification of 2-(phenyl)-1,3,2-dioxaborolane. *Journal of Organometallic Chemistry* **692**: 784–790. https://doi.org/10.1016/j.jorganchem.2006.10.013

Ruiz-Molina D, Saiz Poseu J, Busque F, Nador F, Mancebo J (2018). The chemistry behind catechol-based adhesion. *Angewandte Chemie International Edition* **58**: 696–714. https://doi.org/10.1002/anie.201801063

Sarna T, Hyde J, Swartz H (1976). Ion-exchange in melanin: An electron spin resonance study with lanthanide probes. *Science* **192**: 1132–1134. https://doi.org/10.1126/science.179142

Sauerwein WAG, Sancey L, Hey-Hawkins E, Kellert M, Panza L et al. (2021). Theranostics in boron neutron capture therapy. *Life* **11**: 330. https://doi.org/10.3390/life11040330

Schubert DM, Smith RA, Visi MZ (2003). Studies of crystalline nonmetal borates. *Glass Technology* **44**: 63–70. *https://www.ingentaconnect.com/content/sgt/gt/2003/00000044/00000002/art00006*

Schwint AE, Monti Hughes A, Garabalino MA, Santa Cruz GA, González SJ et al. (2020). Clinical veterinary boron neutron capture therapy (BNCT). Studies in dogs with head and neck cancer: Bridging the gap between translational and clinical studies. *Biology* **9**: 327. https://doi.org/10.3390/biology9100327

Schwint AE, Trivillin VA (2015). "Close-to-ideal" tumor boron targeting for boron neutron capture therapy is possible with less-than-ideal boron carriers approved for use in humans. *Therapeutic Delivery* **6**: 269–272. https://doi.org/10.4155/tde.14.108

Scognamiglio F, Travan A, Turco G, Borgogna M, Marsich E, Pasqua M, Paoletti S, Donati I (2017). Adhesive coatings based on melanin-like nanoparticles for surgical membranes. *Colloids and Surfaces B: Biointerfaces* **155**: 553–559. https://doi.org/10.1016/j.colsurfb.2017.04.057

Stockert JC (2021). Melanin and melanoma: Updating molecular structure and photothermal therapy. *InVet* **23**: 1–15.

Stockert JC (2022). Molecular modeling of phenyl-boronic acids and catechol-borate esters: A mechanistic rationale for boron binding to melanin catechols, regarding the ^{10}boron neutron-capture therapy of melanoma. *Annual Reviews and Research* **8**: 555726. https://doi.org/10.19080/ARR.2022.08.555726

Stockert JC, Blázquez-Castro A (2017). *Fluorescence Microscopy in Life Sciences*. E-Book. Sharjah, United Arab Emirates: Bentham Science Publishers.

Stockert JC, Blázquez-Castro A (2022). Biomedical overview of melanin. 2. Updating molecular modeling, synthesis mechanism, and supramolecular properties regarding melanoma therapy. *BIOCELL* **46**: 1391–1415. https://doi.org/10.32604/biocell.2022.019493

Stockert JC, Espada J, Blázquez-Castro A (2022). Melanin-binding colorants: Updating molecular modeling, staining and labeling mechanisms, and biomedical perspectives. *Colorants* **1**: 91–120. https://doi.org/10.3390/colorants1010007

Stockert JC, Felix-Pozzi MN (2023). Updating curvature of graphitic materials: Molecular modeling studies on the spiral structure of graphene and eumelanin models. *Advances in Biology* **2**: 173–205. ISBN: 979-8-88697-422-5.

Stockert JC, Juarranz A, Villanueva A, Nonell S, Horobin RW et al. (2004). Photodynamic therapy: Selective uptake of photosensitizing drugs into tumor cells. *Current Topics in Pharmacology* **8**: 185–217.

Tsuyumoto I, Oshio T, Katayama K (2007). Preparation of highly concentrated aqueous solution of sodium borate. *Inorganic Chemistry Communications* **10**: 20–22. https://doi.org/10.1016/j.inoche.2006.08.019

Udenfriend S (1962). *Fluorescence Assay in Biology and Medicine,* pp. 388–394. New York, London: Academic Press.

Villanueva A, Vidania R, Stockert JC, Cañete M, Juarranz A (2003). Photodynamic effects on cultured tumor cells: Cytoskeleton alterations and cell death mechanisms. In: Nalwa HS (ed.), *Handbook of Photochemistry and Photobiology*, vol. 4, pp. 79–117. California: American Scientific Publishers.

Wittig A, Arlinghaus HF, Kriegeskotte C, Moss RL, Appelman K, Schmid KW, Sauerwein WAG (2008b). Laser postionization secondary neutral mass spectrometry in tissue: A powerful tool for elemental and molecular imaging in the development of targeted drugs. *Molecular Cancer Therapy* **7**: 1763–1771. https://doi.org/10.1158/1535-7163.MCT-08-0191

Wittig A, Michel J, Moss RL, Stecher-Rasmussen F, Arlinghaus HF et al. (2008a). Boron analysis and boron imaging in biological materials for boron neutron capture therapy (BNCT). *Critical Reviews in Oncology and Hematology* **68**: 66–90. https://doi.org/10.1016/j.critrevonc.2008.03.004

Yan J, Fang H, Wang B (2005). Boronolectins and fluorescent boronolectins: An examination of the detailed chemistry issues important for the design. *Medicinal Research Reviews* **25**: 490–520. https://doi.org/10.1002/(ISSN)1098-1128

Yang W, Yan J, Springsteen G, Deeter S, Wang B (2003). A novel type of fluorescent boronic acid that shows large fluorescence intensity changes upon binding with a carbohydrate in aqueous solution at physiological pH. *Bioorganic and Medicinal Chemistry Letters* **13**: 1019–1022. https://doi.org/10.1016/S0960-894X(03)00086-6

Yasunobu KT, Norris ER (1957). Mechanism of borate inhibition of diphenol oxidation by tyrosinase. *Journal of Biological Chemistry* **227**: 473–482. https://doi.org/10.1016/S0021-9258(18)70830-2

Yoshino K, Kotaka M, Okamoto M, Kakihana H (1979). 11B-NMR study of the complex formation of borate with catechol and L-DOPA. *Bulletin of the Chemical Society Japan* **52**: 3005–3009. https://doi.org/10.1246/bcsj.52.3005

Yoshino K, Mishima Y, Kimura M (1997). Capture of p-boronophenylalanine in malignant melanoma cells by complex formation with melanin monomers, DOPA, DHI and DHICA. In: Larsson B, Crawford J, Weinreich R (eds.), *Advances in Neutron Capture Therapy,* vol. II, pp. 234–238. Amsterdam: Elsevier.